Catalysis Today 158 (2010) 354–360

Contents lists available at ScienceDirect

Catalysis Today

journal homepage: www.elsevier.com/locate/cattod

Effect of pH on electrocatalytic property of supported PtRu catalysts in proton exchange membrane fuel cell

Min-Sik Kim [a], Sinmuk Lim [a], Nitin K. Chaudhari [a], Baizeng Fang [a], Tea-Sung Bae [b], Jong-Sung Yu [a,*]

[a] Department of Advanced Materials Chemistry, BK21 Research Team, Korea University, 208 Seochang, Jochiwon, ChungNam 339-700, Republic of Korea
[b] Korea Basic Science Institute, Jeonju, Republic of Korea

ARTICLE INFO

Keywords:
Homogeneous deposition
Urea
Electrocatalyst
Anode
Proton exchange membrane fuel cell

ABSTRACT

In this study, urea-assisted homogeneous deposition (HD) strategy is employed to synthesize Vulcan XC-72 (VC)-supported Pt–Ru (40 wt%) catalysts under various initial pH conditions. In situ generation of hydroxide ions through hydrolysis of urea at elevated temperature results in HD of Pt–Ru species on the VC support. In addition, it has been found that the initial pH value in the starting solution has significant influence on the Pt–Ru metal particle size and the catalytic activity of the supported Pt–Ru catalyst. Under most pH values investigated (i.e., higher than 5–6), the VC-supported Pt–Ru catalysts prepared by the HD approach have shown smaller metal particle size with better particle dispersion and demonstrated greatly improved anode catalyst performance over the one prepared by impregnation-$NaBH_4$ reduction at pH 7–8 in proton exchange membrane fuel cell. The results presented in this work highlight that highly efficient Pt-based catalysts can be prepared by the HD strategy through the control of the initial pH value in the starting solution.

1. Introduction

Since the past decade proton exchange membrane fuel cell (PEMFC) has been receiving enormous attention as future energy source for a range of applications in low/zero-emission electric vehicles, distributed home power generators, and as a power source for small portable electronic devices due to their high power density, relatively quick startup, rapid response to varying metal loading, and relatively low operating temperatures [1–5].

At present, Pt–Ru alloy and Pt metal are commonly used as anode and cathode catalysts, respectively, for the PEMFC. However, Pt and Ru are noble metals and have low natural abundance, a major shortcoming for practical applications thus escalating the manufacturing cost and restricting its commercialization. For the effective use of these noble metals as catalysts, they have to be well dispersed as small particles on the conductive supporting materials such as porous carbon to enhance the cell performance. It is well known that the catalytic activity is strongly governed by the size and dispersion of catalytic particles [6]. To date, voluminous work has been carried out exploring the possibilities to minimize the usage of noble metals by maximizing their catalytic utilization, which can be achieved by reducing the metal particle size and improving particle dispersion on the catalyst support [7]. Various synthesis strategies such as impregnation [8,9], microemulsion [10,11], ion exchange [12], colloidal [13,14] and irradiation method [15,16] have been employed to prepare bimetallic Pt–Ru catalysts. However, inadequate control of particle morphology and ineffective removal of surfactants limit the efficacy of these synthesis routes. As a result, novel, easy and reliable synthesis routes are of enormous significance to prepare monodisperse and stoichiometrically uniform Pt–Ru nanoparticles to enhance the catalyst performance of the PEMFC. In accordance to that, the present work was undertaken with an objective of investigating a simple reliable procedure for the synthesis of Vulcan XC-72 (VC)-supported high metal loading Pt–Ru catalyst. Urea-assisted homogeneous deposition (HD) method has been applied in the preparation of uniform well-dispersed metal catalysts (such as Au, Pt, Ru) on oxide supports with very low metal loading (less than 5 wt%) for various organic reactions [17–24]. Recently, a HD strategy coupled with ethylene glycol (EG) reduction has been developed to synthesize VC-supported high loading of Pt catalysts [25]. Although the HD-EG technique proved to be efficient in preparation of Pt catalysts with smaller Pt nanoparticle size and more uniform particle distribution compared with those by impregnation-$NaBH_4$ reduction or EG-irradiation method, the pH values adjustment through urea hydrolysis at elevated temperature seems to be limited, and a pH value lower than 5 or higher than 9 could not be easily achieved by the use of urea only. As we know, pH value in the initial solution plays an important role in controlling the particle size and distribution of metal nanoparticles of the supported catalysts. Therefore, it

* Corresponding author. Tel.: +82 41 860 1494; fax: +82 41 867 5396.
E-mail address: jsyu212@korea.ac.kr (J.-S. Yu).

0920-5861/$ – see front matter © 2010 Elsevier B.V. All rights reserved.
doi:10.1016/j.cattod.2010.04.037

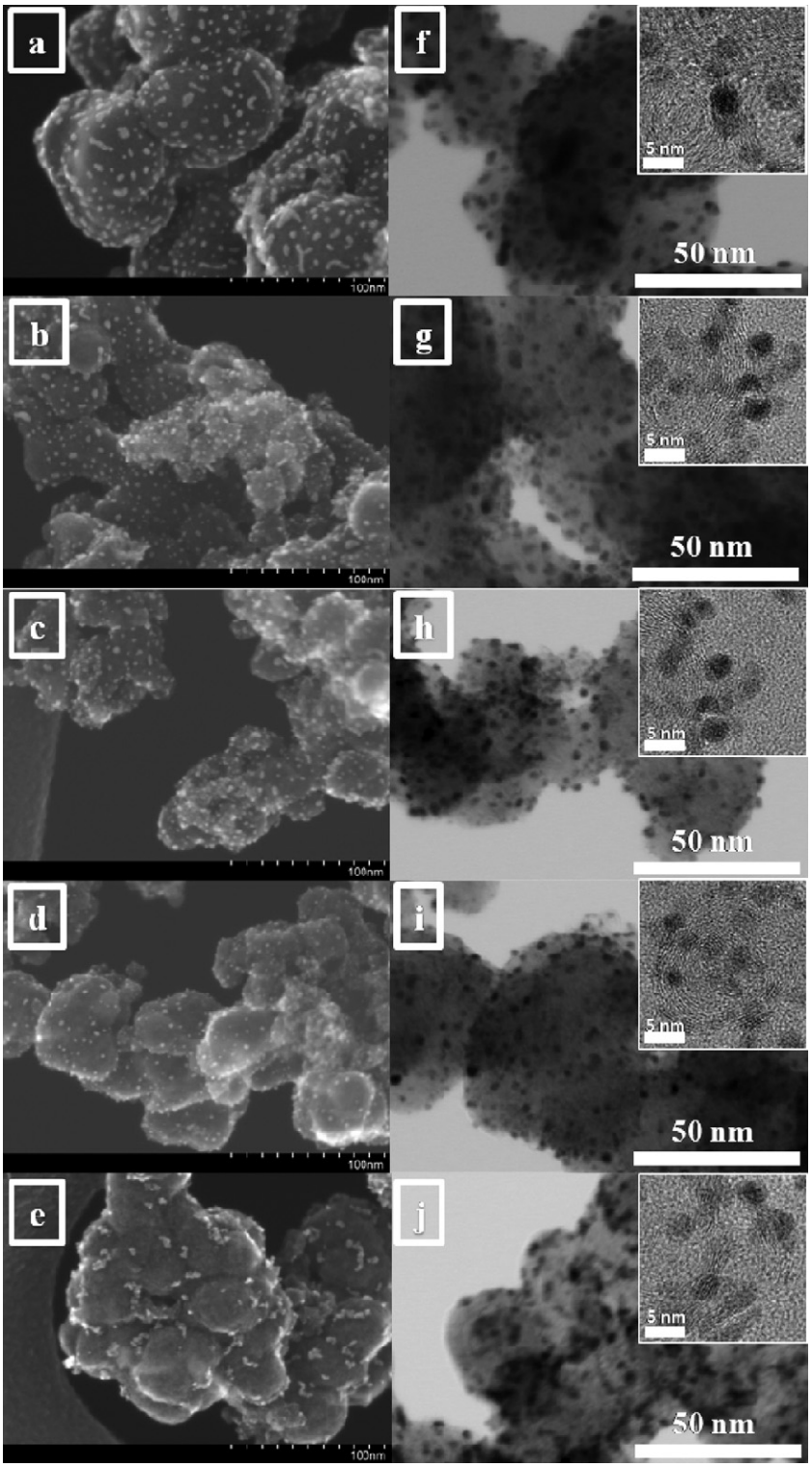

Fig. 1. HR-SEM and HR-TEM images of 40 wt% PtRu/VC catalysts (inset: high magnification HR-TEM images): (a and f) Pt–Ru/VC-U1 (pH 3–4), (b and g) Pt–Ru/VC-U2 (pH 5–6), (c and h) Pt–Ru/VC-U3 (pH 7–8), (d and i) Pt–Ru/VC-U4 (pH 9–10) and (e and j) Pt–Ru/VC-$NaBH_4$ (pH 7–8).

is significant and necessary to examine systematically the influence of pH in the initial solution on the morphology, distribution and catalytic activity of the supported catalysts. In this report, we synthesized comparatively high metal loading (i.e., 40 wt%) PtRu/VC catalysts through the modification of the HD method. Namely, a H_2 reduction step was taken after the HD step. The HD step permits gradual and homogeneous generation of hydroxide ions throughout the whole aqueous solution through the hydrolysis reaction of urea (i.e., $CO(NH_2)_2 + 3H_2O \rightarrow 2NH_4^+ + CO_2 + 2OH^-$), avoiding sudden local increase in pH value and excessively rapid precipitation of metal hydroxide in the bulk solution. After the HD step for the precipitation of the PtRu hydroxide colloids, the supported high metal loading Pt–Ru/VC catalysts were successfully prepared by thermal reduction under flowing hydrogen gas. The influences of pH values in the starting solutions on Pt–Ru particle size and dispersion on the carbon support were investigated. It was found that Pt–Ru nanopar-

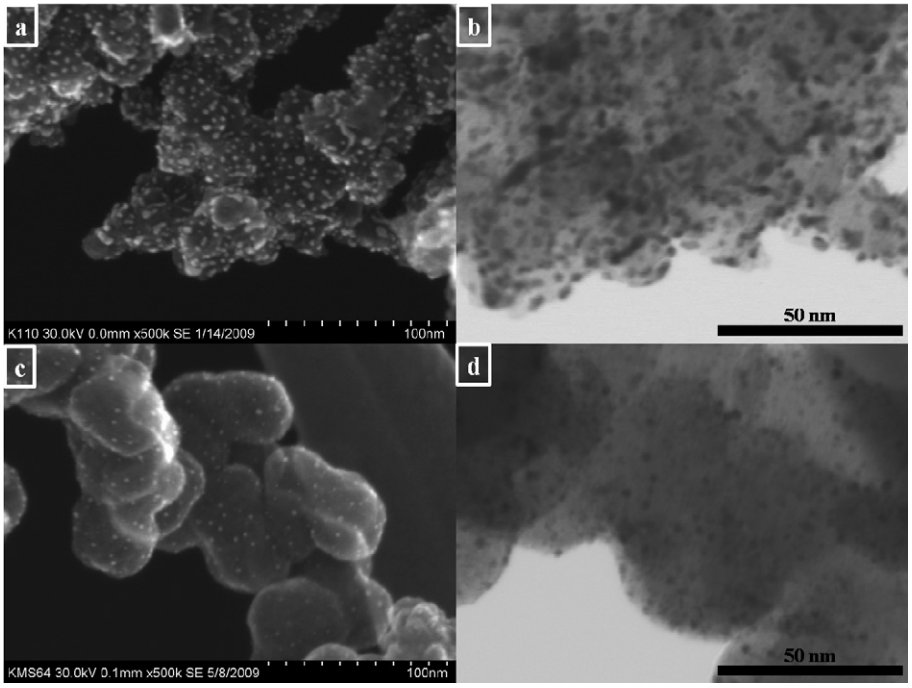

Fig. 2. HR-SEM and HR-TEM images of Pt–Ru/VC catalysts (HD-H_2): (a and b) 60 wt% Pt–Ru/VC and (c and d) 20 wt% Pt–Ru/VC prepared at pH 9–10.

ticle sizes and their catalytic activities as anode Pt–Ru/VC catalysts depend greatly on the pH values in the starting solution. Interestingly, the Pt–Ru/VC catalysts synthesized under high pH values by the modified HD method (i.e., HD-H_2) have shown better dispersion with smaller particle size and thus demonstrated enhanced catalytic activity and PEMFC performance compared with the one prepared by the conventional impregnation-$NaBH_4$ reduction.

2. Experimental

2.1. Synthesis of Pt–Ru/VC catalysts

$H_2PtCl_6{\cdot}6H_2O$ (Kojima) and $RuCl_3$ (Aldrich) were used as metal precursors and Vulcan XC-72 (VC) carbon black (Cabot) as support for the synthesis of catalyst. Urea (Aldrich) and VC were used as received.

Pt–Ru/VC (40 wt%) catalysts were prepared by two different synthesis methods, namely, impregnation-$NaBH_4$ reduction and HD-H_2 reduction. The catalysts thus prepared were denoted as Pt–Ru (40 wt%)/VC-$NaBH_4$ and Pt–Ru (40 wt%)/VC-U, respectively. The details on the $NaBH_4$ approach at pH of 7–8 can be found elsewhere [26,27].

In a typical HD-H_2 synthesis, equimolar amounts of hydrogen hexachloroplatinate and ruthenium chloride were dissolved in deionized water with vigorous stirring. The urea solution was prepared by dissolving appropriate amount of urea (molar ratio of urea to metal was ~20) in deionized water with stirring. The above both solutions were mixed and stirred for 30 min at ambient temperature. The VC was suspended in deionized water and then mechanically stirred to obtain homogeneous carbon solution. The resultant carbon solution was mixed with the previously prepared metal salt–urea mixture solution at controlled pH values (3–4, 5–6, 7–8 or 9–10) and then stirred for 1 h at 90 °C. The resulting Pt–Ru (40 wt%)/VC-U catalysts were denoted as Pt–Ru/VC-U1, Pt–Ru/VC-U2, Pt–Ru/VC-U3 and Pt–Ru/VC-U4, respectively. The initial pH of the mixture solution was around 3–4 and adjusted to the controlled value with 3.0 M NaOH solution. The as-obtained solution was cooled to room temperature, filtered, thoroughly washed with deionized water and dried in a vacuum oven at 80 °C for overnight. After drying, the residue was heated in a tube furnace at 300 °C under flowing H_2 for 1 h. In addition to the metal loading of 40 wt%, Pt–Ru catalysts with various metal loadings, i.e., 20 and 60 wt% were also prepared by HD-H_2 strategy with the initial pH of the mixture solution of 9–10 for comparison. Actual metal loadings of the VC-supported Pt–Ru catalysts were roughly determined by the thermogravimetric analysis (TGA). TGA analysis was carried out using a SCINCO TG 1000 Model under a flow of dry air. Sample weight was in the range of 10–20 mg with heating rate of 15 °C/min.

2.2. Characterization

As-synthesized supported catalysts were characterized using various techniques such as high resolution-transmission electron microscopes (HR-TEM), high resolution-scanning electron microscopes (HR-SEM), and X-ray diffraction (XRD) analysis. HR-TEM images were obtained by using transmission electron microscope (JEM 2200-FS) operated at 200 kV and HR-SEM images were obtained by using ultra high resolution-scanning electron microscope (Hitachi S-5500) operated at 30 kV. The XRD patterns were recorded by using a Rigaku diffractometer with Cu Kα radiation at a scan rate of 4°/min at 40 kV and 20 mA.

2.3. Half-cell tests

Half-cell (i.e., three-electrode electrochemical cell) was constructed and CO stripping voltammogram measurements conducted to examine electrochemical surface area (ESA) of the in-house Pt–Ru catalysts. Pt gauze was used as a counter electrode and Ag/AgCl as a reference one. The working electrode was a thin layer of Nafion-impregnated catalyst cast on a glassy carbon disk (3 mm in diameter) embedded in a Teflon cylinder. Preparation method for the working electrode was described elsewhere [28]. The catalyst loading in the working electrode was 0.2 mg Pt/cm^2. Before starting CO stripping, the electrolyte (i.e., 0.5 M H_2SO_4) was purged by N_2 for 20 min. After that, a mixture gas of CO and N_2 (containing 20% (v/v) CO) was introduced for 15 min while the

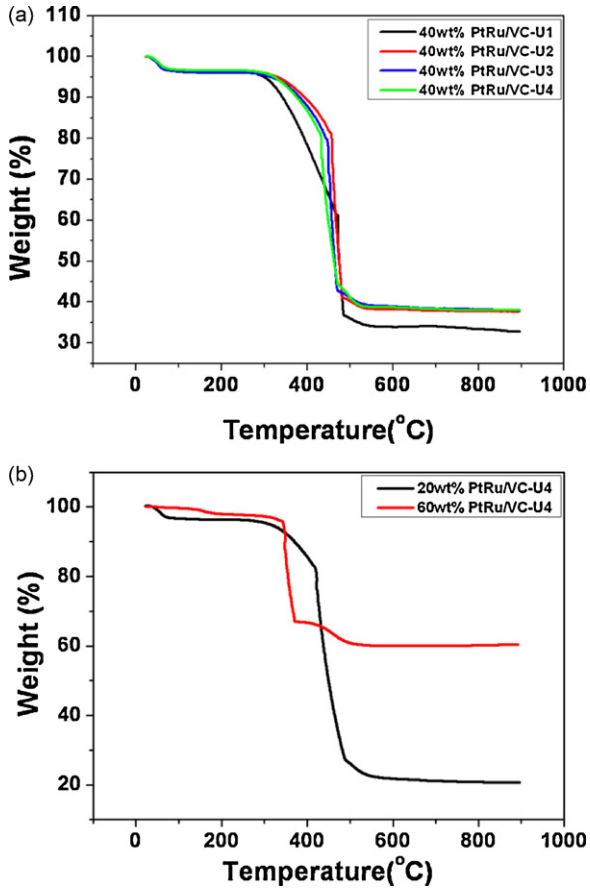

Fig. 3. Thermogravimetric analysis curves for the various Pt–Ru/VC-U*x* catalysts prepared using HD-H_2 method.

working electrode was kept at a potential of −0.12 V versus Ag/AgCl reference electrode. Next, the dissolved CO in the electrolyte was removed by bubbling N_2 for 20 min, and the stripping voltammograms were recorded at a scan rate of 25 mV/s. All the recorded currents are normalized by the mass percentage of platinum in the catalysts.

2.4. Single-cell tests

Fuel cell polarization performance was evaluated using single cell with a 6.25 cm^2 cross-sectional catalyst area and conducted with WFCTS fuel cell test station (WonA Tech Co., Ltd, Korea). H_2 and O_2 gases were supplied to the anode and cathode at flow rates of 200 and 500 ml/min, respectively, with zero back pressures. Before feeding to the cell, H_2 and O_2 gases had been humidified at a temperature of 15 °C higher than the cell's operating temperature.

The membrane electrode assembly (MEA) was made by hot-pressing (135 °C, 2000 psi for 5 min). Pretreated Nafion-115 (Du-Pont) membrane was sandwiched between the anode and cathode, which had been prepared by painting a desired amount of supported catalyst ink on a teflonized carbon paper (TGPH-090) and dried in an oven at 70 °C for 1 h. The catalyst ink was prepared by mixing 100 mg of catalyst with 0.763 ml of 5 wt% Nafion solution and kept on stirring prior to use. The catalyst loadings at anode (40 wt% PtRu/VC) and cathode (20 wt% Pt/VC from E-TEK) were 0.4 mg Pt–Ru/cm^2 and 0.4 mg Pt/cm^2, respectively. The Nafion-115 membrane used was pretreated first by boiling in 3 wt% H_2O_2 for 1 h followed by boiling again in 0.5 M H_2SO_4 for 1 h. The single-cell test fixture comprised of two steel end plates

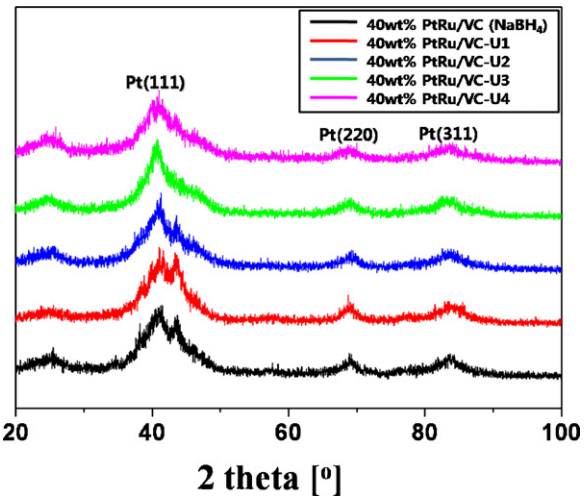

Fig. 4. The XRD patterns of 40 wt% Pt–Ru/VC catalysts synthesized using HD-H_2 at various pH values and Pt–Ru/VC-$NaBH_4$ catalyst.

and two graphite plates with rib-channel patterns allowing the passage of hydrogen gas to the anode and oxygen gas to the cathode. Measurements for fuel cell power test of each sample were repeated thrice for reproducibility at the same experimental conditions.

For evaluation of electrochemical stability of the Pt–Ru catalysts, the chronoamperometric tests were conducted at 0.75 V for 4 h.

3. Results and discussion

Fig. 1 shows the representative HR-SEM and HR-TEM images for 40 wt% Pt–Ru/VC-U catalysts prepared under various initial pH conditions and for the Pt–Ru/VC-$NaBH_4$ catalyst prepared at pH of 7–8. On the whole, all of the Pt–Ru/VC-U catalysts show uniform Pt–Ru dispersion on the carbon support with narrow particle size distribution. The average metal particle sizes were determined by measuring the diameters of near 100 nanoparticles found in an arbitrarily chosen area in enlarged photographs. The average metal particle size was found to be 3.6 nm (standard deviation (SD): 0.31), 3.2 nm (SD: 0.25), 3.0 nm (SD: 0.21), and 2.7 nm (SD: 0.19) in diameter for the Pt–Ru/VC-U1, Pt–Ru/VC-U2, Pt–Ru/VC-U3, and Pt–Ru/VC-U4, respectively. The Pt–Ru/VC-U1 catalyst shows sporadically larger metal particles probably due to agglomeration. The most uniform and well-dispersed metal nanoparticles were found for the Pt–Ru/VC-U4 catalyst, which was synthesized in relatively basic condition (i.e., pH of 9–10). In contrast, inferior particle size distribution is observed in Fig. 1 for the Pt–Ru (40 wt%)/VC-$NaBH_4$ along with larger mean particle size and some metal agglomeration. The supported Pt–Ru nanoparticles have a wider particle size distribution of ca. 2.3–4.7 nm, and the mean particle size was estimated to be around ca. 3.5 nm.

HR-SEM/TEM images shown in Fig. 2 reveal that through the HD-H_2 synthesis strategy Pt–Ru catalysts can be prepared with relatively low metal loading (i.e., 20 wt%) but with smaller metal particle size along with more uniform particle distribution compared with Pt–Ru (40 wt%)/VC catalyst. Particularly important and interestingly, with a higher metal loading, i.e., 60 wt%, the Pt–Ru catalyst still exhibits uniform particle distribution except very few and light particle agglomeration observed somewhere, implying the effectiveness of HD-H_2 synthesis strategy.

TGA data shown in Fig. 3 reveal that the metal loadings in all the catalysts are close to their nominal values, implying the Pt and Ru complex ions in the initial metal salt solutions have been successfully reduced to metallic Pt and Ru. Interestingly, for

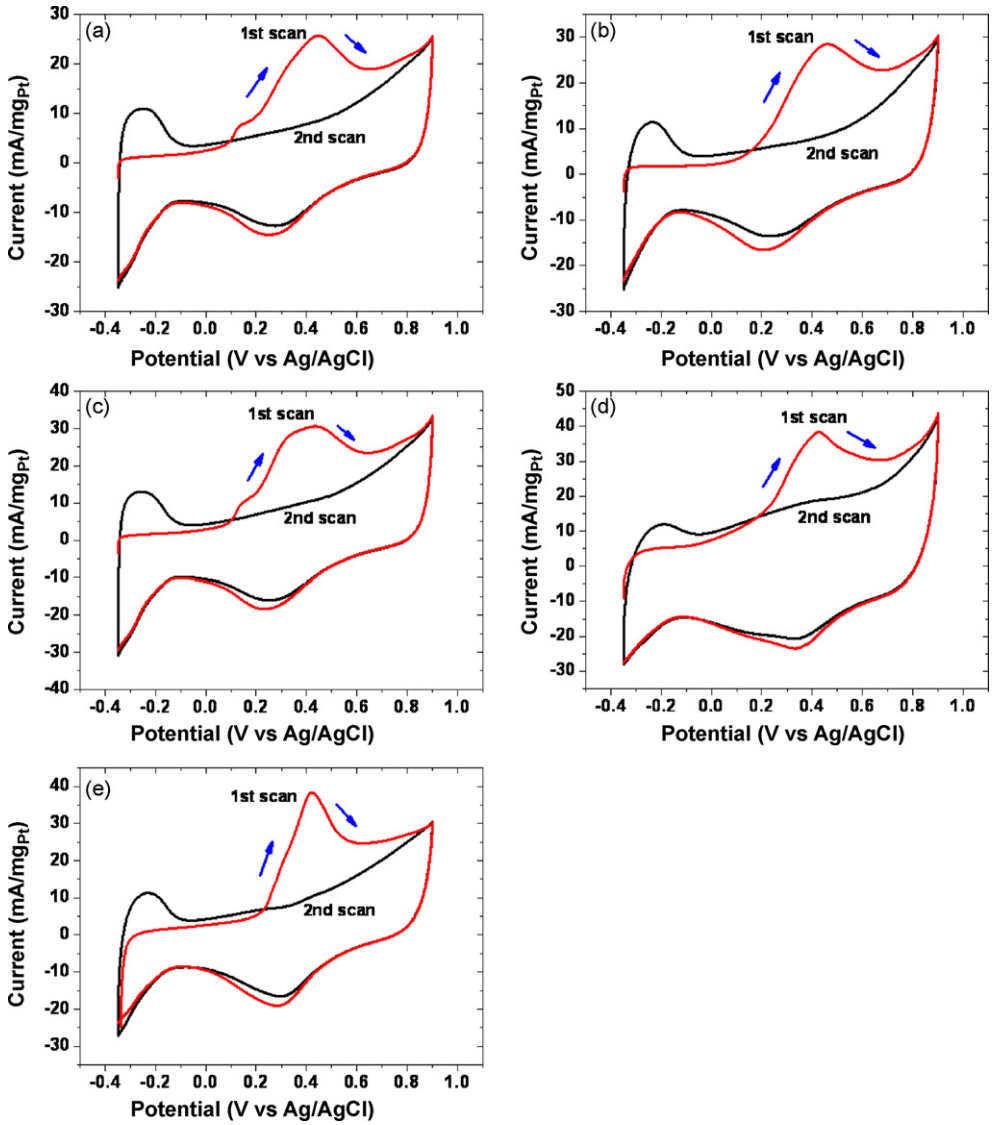

Fig. 5. CO stripping voltammograms for the various Pt–Ru (40 wt%)/VC catalysts ((a) $NaBH_4$, (b) U1 (pH 3–4), (c) U2 (pH 5–6), (d) U3 (pH 7–8) and (e) U4 (pH 9–10)) in 0.5 M H_2SO_4 at 25 mV/s.

PtRu/VC-U1, the metal loading was found to be 35 wt%, slightly less than the nominal 40 wt%, which indicates that hydroxide ions generated only by urea hydrolysis may not be sufficient to form stable PtRu hydroxide precipitation in this initial low pH condition.

Fig. 4 demonstrates characteristic XRD patterns for the Pt–Ru (40 wt%)/VC catalysts synthesized at various pH values using urea and for Pt–Ru (40 wt%)/VC catalyst synthesized using $NaBH_4$ as a reducing agent. The broad signal located at ca. 24.5° in the XRD patterns is associated with the VC support. Pt shows characteristic peaks of face-centered cubic (FCC) crystallinity (JCPDS-ICDD, card no. 04-802) with the planes (1 1 1), (2 2 0) and (3 1 1) at 2θ values of ca. 39.8°, 67.8°, and 81.2°, respectively. All the XRD patterns indicate that the Pt–Ru/VC alloy catalysts reveal principally single-phase disordered structures of Pt. Compared to the reflections in pure Pt, the diffraction peaks for the Pt–Ru alloy catalysts have slightly shifted to higher 2θ values of ca. 41.0°, 68.9°, and 83.6° for (1 1 1), (2 2 0) and (3 1 1), respectively, as shown in Fig. 4, indicating the formation of an alloy involving the incorporation of Ru atom into the FCC structure of Pt. The average particle sizes calculated from a (2 2 0) X-ray diffraction peak of Pt FCC lattice by using the Scherrer equation [29] are in good agreement with the values estimated from HR-TEM images. The data obtained from the XRD analysis are summarized in Table 1. It was observed that the particle size in the Pt–Ru/VC catalyst (HP-H_2) decreases with the increase in the pH of the starting solution, which suggests that the pH of the solution has significant effect on the metal particle size and the particle distribution in agreement of previous works [14,30–35]. Salgado et al. [35] reported that the mean particle size of the Pt–Co/C prepared in acid medium is larger than that of the catalyst prepared in basic medium. The decrease in

Table 1
Particle size and fuel cell performance for the Pt–Ru (40 wt%)/VC catalysts prepared by the HD-H_2 under various pH values or by $NaBH_4$ method.

Sample	pH	Pt–Ru particle size (nm)[a]	Maximum power (W)[b]	ESA (m^2/g)
Pt–Ru/VC-$NaBH_4$	7–8	3.5	2.17	35
Pt–Ru/VC-U1	3–4	3.6	2.13	36
Pt–Ru/VC-U2	5–6	3.1	2.58	43
Pt–Ru/VC-U3	7–8	3.0	2.63	45
Pt–Ru/VC-U4	9–10	2.6	2.81	55

[a] Average particle size (calculated from XRD patterns).
[b] Average maximum power of single-cell tests (cathode: O_2, anode: H_2, 60 °C).

size of the metal particle with increasing pH value is probably attributable to the following reasons. (i) In a solution with higher pH, more OH^- ions are provided, and in this situation, more Cl^- in $[PtCl_6]^{2-}$ complex ions can be replaced by OH^- through a chemical reaction like that $[PtCl_6]^{2-} + xOH^- \rightarrow [Pt(OH)_xCl_{6-x}]^{2-} + xCl^-$. Apparently, the size of $[Pt(OH)_xCl_{6-x}]^{2-}$ should be smaller than $[PtCl_6]^{2-}$ due to the smaller ionic radius of OH^- compared with Cl^-. The smaller the size of deposited Pt(IV) complex on the VC, the smaller the size of metal Pt atom and Pt–Ru alloy during the H_2 reduction. (ii) In a solution with lower pH particularly in an acidic aqueous medium, due to insufficient supply of OH^- even after the urea hydrolysis, part of Pt and Ru hydroxide colloids might be involved in a so-called precipitation-dissolution process, resulting in uneven growth and larger particulate size of Pt and Ru hydroxide colloids. While in a solution with higher pH value, less or no Pt and Ru hydroxide colloids undergo such precipitation-dissolution process, ensuring the even growth of the Pt and Ru hydroxide particulate on their nucleation sites. In this case, in situ generation of OH^- through hydrolysis of urea not only provides more OH^-, which favors and stabilizes the formation of metal hydroxide on the carbon support, but also protects the metal hydroxide particulates from agglomeration in the precipitation process due to the presence of excess amount of hydroxide ions in the solution.

Efficient removal of the poisoning species such as CO from the catalyst is an important measure for evaluating the catalyst property and determining ESA for Pt–Ru catalyst. The CO stripping voltammograms for the various Pt–Ru/VC catalysts are shown in Fig. 5. In all the cases, the broad anodic peak observed during the first potential-positively going scan disappears in the second scan, indicating that the adsorbed CO has been completely oxidized during the first forward scan. For most of Pt–Ru/VC catalysts prepared by HD-H_2 method (i.e., pH greater than 5–6), the peak intensity of CO electro-oxidation is larger than that observed for the Pt–Ru/VC ($NaBH_4$), implying the larger ESAs for the HD-H_2 catalysts. With the assumption of 420 $\mu C/cm^2$ as the oxidation charge for one monolayer of CO on a smooth Pt surface and after the subtraction of the background current of the second scan, ESAs were determined using the CO oxidation charge to be 36, 43, 45, 55 and 35 m^2/g for Pt in the Pt–Ru/VC-U1, U2, U3, U4 and $NaBH_4$, respectively. Compared with $NaBH_4$ catalyst, higher ESAs for the HD-H_2 catalysts suggest better utilization efficiency due to smaller Pt–Ru nanoparticles and better particle distribution.

The fuel cell polarization performance plots for the various Pt–Ru (40 wt%)/VC catalysts are shown in Fig. 6a. Evidently, most Pt–Ru (40 wt%)/VC-U catalysts prepared at relatively high pH values (i.e., greater than 5) reveal a higher open circuit voltage than that for the Pt–Ru (40 wt%)/VC-$NaBH_4$, which is probably related to the characteristics of the catalysts such as smaller metal particle size and more uniform particle distribution of the former. Furthermore, they also exhibit higher anodic catalytic activities, which can be clearly observed at low polarization current density of smaller than 0.05 A/cm^2. At the identical current density, smaller polarization voltage losses observed for the Pt–Ru (40 wt%)/VC-U catalysts are mainly attributable to the faster anodic polarization reaction taken place on the catalyst electrodes. The maximum power measured is 2.17 W for Pt–Ru/VC-$NaBH_4$, 2.13 W for Pt–Ru/VC-U1, 2.58 W for Pt–Ru/VC-U2, 2.63 W for Pt–Ru/VC-U3, and 2.81 W for Pt–Ru/VC-U4. Particle sizes, ESAs and the maximum power delivered for the various VC-supported Pt–Ru (40 wt%) catalysts are summarized in Table 1, and shown in Fig. 6b. Apparently, in most cases (i.e., for the catalysts prepared at pH values of higher than 5–6), the Pt–Ru (40 wt%)/VC-U catalysts demonstrate higher power than the one prepared by the conventional impregnation-$NaBH_4$ reduction under the identical test condition. The Pt–Ru/VC-U4 synthesized at pH 9–10 shows the highest power, which is 30% higher than the one prepared by $NaBH_4$ reduction. As shown in Fig. 6b for the Pt–Ru/VC-U catalysts, the fuel cell power delivery illustrates an increasing trend with the increasing pH, which mainly results from the decrease in metal particles size along with the improved particle dispersion on the VC support. Fig. 6c shows the chronoamperometry data recorded at a constant voltage of 0.75 V for the various Pt–Ru (40 wt%) anode catalysts. It was found that most Pt–Ru/VC (HD-H_2) catalysts exhibit both higher initial and higher final current response than the Pt–Ru/VC ($NaBH_4$), suggesting that these catalysts are more active towards H_2 oxidation than Pt–Ru/VC ($NaBH_4$), resulting from the smaller Pt–Ru particle size and more uniform particle distribution.

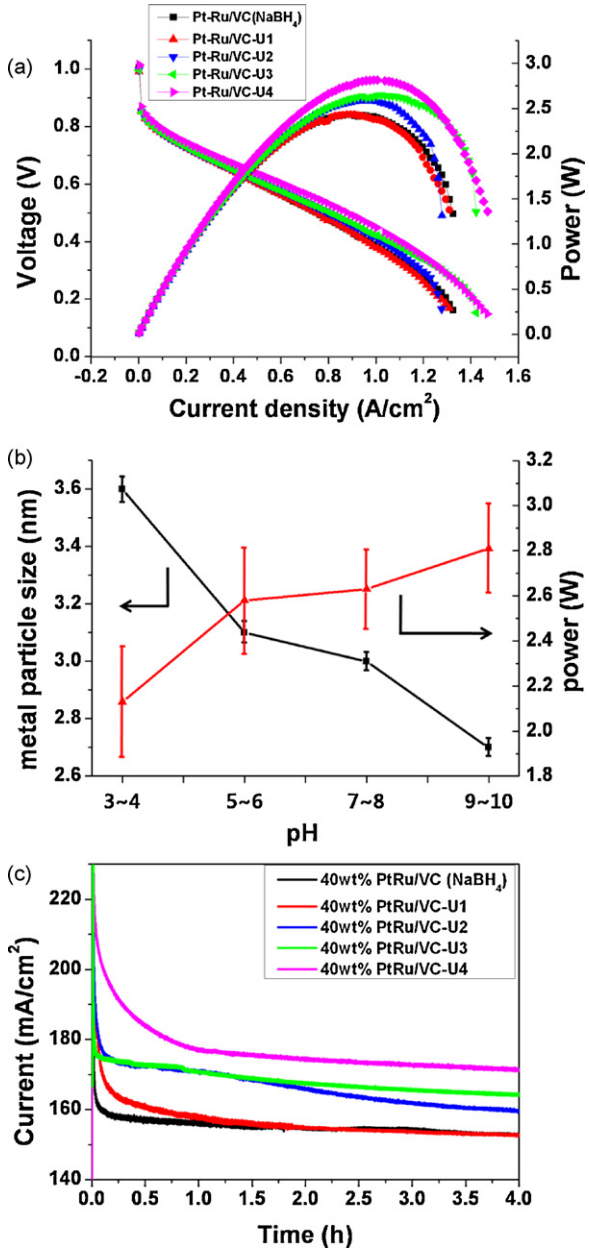

Fig. 6. (a) The polarization and power curves for PEMFC using 40 wt% Pt–Ru/VC catalysts as anode and a commercial E-TEK Pt (20 wt%)/VC catalyst as cathode. (b) Average particle sizes with standard deviation given by length of vertical line (■) of the Pt–Ru/VC-U catalysts and fuel cell power with error bar (▲) shown against pH value. (c) Chronoamperograms obtained at 0.75 V for the various Pt–Ru (40 wt%) catalysts.

4. Conclusions

In the present work, a simple, reliable and inexpensive procedure based on a modified HD method using urea has been described for the synthesis of 40 wt% metal loading of Pt–Ru/VC catalysts. It was found that the pH of the starting solution significantly influences the Pt–Ru metal particle size and the particle dispersion on the carbon support, which are critically related to the PEMFC performance as well. The metal particle size decreased with the increasing pH, which results in the increase in the fuel cell power delivery. At most of the cases especially at high pH values, the in-house Pt–Ru (40 wt%)/VC-U catalysts have demonstrated greatly enhanced catalytic activity and fuel cell performance compared with the one prepared by the conventional impregnation-$NaBH_4$ reduction. Further work on synthesis and electrochemical activity of Pt-based catalysts is under progress with different support and various metals loadings.

Acknowledgements

The authors thank 2009 Korea Institute for Advancement of Technology (KIAT) through the Human Resource Training Project for Regional Innovation and WCU Research Program for financial support. Special thank is given to KBSI for HR-SEM, HR-TEM (Jeonju), and XRD (Daejeon) measurements.

References

[1] N.A. Oliveira, E.G. Franco, E. Arico, M. Linardi, E.R. Gonzalez, J. Eur. Ceram. Soc. 23 (2003) 2987.
[2] T. Toda, H. Igarashi, H. Uchida, M. Watanabe, J. Electrochem. Soc. 146 (1999) 3750.
[3] T.E. Springer, T.A. Zawodzinski, S. Gottesfeld, J. Electrochem. Soc. 138 (1991) 2334.
[4] S.J.C. Cleghorn, X. Ren, T.E. Springer, M.S. Wilson, T.A. Zawodzinski, S. Gottesfeld, Int. J. Hydrogen Energy 22 (1997) 1137.
[5] R. Service, Science 296 (2002) 1222.
[6] S.B. Yoon, B. Fang, M. Kim, J.H. Kim, J.-S. Yu, in: G. Wilde (Ed.), Nanostructured Materials, Elsevier, 2009, pp. 173–231 (Chapter 4).
[7] S. Litster, G. McLean, J. Power Sources 136 (2004) C41.
[8] J.-S. Yu, S. Kang, S.B. Yoon, G.S. Chai, J. Am. Chem. Soc. 124 (2002) 9382.
[9] A.L. Mohana, S. Ramaprabhu, J. Phys. Chem. C 111 (2007) 16138.
[10] J. Mathiyarasu, L.N. Phani, J. Electrochem. Soc. 154 (2007) B110.
[11] Y. Qianm, W. Wen, P.A. Adcock, Z. Jiang, N. Hakim, M.S. Saha, S. Mukerjee, J. Phys. Chem. C 112 (2008) 116.
[12] D. Thompsett, in: G. Hoogers (Ed.), Fuel Cell Technology Book, CRC Press, LLC, New York, 2003 (Chapter 6).
[13] C. Wang, M. Waje, X. Wang, J.M. Tang, R.C. Haddon, Y. Yan, Nano Lett. 4 (2004) 345.
[14] C. Bock, C. Paquet, M. Couillard, G.A. Botton, B.R. MacDougall, J. Am. Chem. Soc. 126 (2004) 8028.
[15] G.S. Chai, B. Fang, J.-S. Yu, Electrochem. Commun. 10 (2008) 1801.
[16] Z.Q. Tian, S.P. Jiang, Y.M. Liang, P.K. Shen, J. Phys. Chem. B 110 (2006) 5343.
[17] R. Zanella, S. Giorgio, C.R. Henry, C. Louis, J. Phys. Chem. B 106 (2002)7634.
[18] M.L. Toebes, M.K. Lee, L.M. Tang, M.H.H. Veld, J.H. Bitter, A.J. Dillen, K.P. Jong, J. Phys. Chem. B 108 (2004) 11611.
[19] S. Chytil, W.R. Glomm, I. Kvande, T. Zhao, J.C. Walmsley, E.A. Blekkan, Top. Catal. 45 (2007) 93.
[20] N.S. Patil, B.S. Uphade, P. Jana, S.K. Bharagava, V.R. Choudhary, J. Catal. 223 (2004) 236.
[21] N.S. Patil, B.S. Uphade, P. Jana, S.K. Bharagava, V.R. Choudhary, Chem. Lett. 33 (2004) 400.
[22] N.S. Patil, B.S. Uphade, D.G. McCulloh, S.K. Bharagava, V.R. Choudhary, Catal. Commun. 5 (2004) 681.
[23] L.A.M. Hermans, J.W. Geus, Stud. Surf. Sci. Catal. 4 (1979) 113.
[24] J.A. van Dillen, J.W. Geus, L.A. Hermans, J. van der Meijden, Proceedings of the 6th International Congress on Catalysis, London, 1976.
[25] B. Fang, N.K. Chaudhari, M.-S. Kim, J.H. Kim, J.-S. Yu, J. Am. Chem. Soc 131 (2009) 15330.
[26] J.H. Kim, B. Fang, M. Kim, J.-S. Yu, Catal. Today 146 (2009) 25.
[27] B. Fang, M. Kim, S. Hwang, J.-S. Yu, Carbon 46 (2008) 876.
[28] J.H. Kim, B. Fang, S.B. Yoon, J.-S. Yu, Appl. Catal. B: Environ. 88 (2009) 368.
[29] B.D. Cullity, Elements of X-ray Diffraction, Addison-Wesley Pub. Inc., New York, 1984 (Chapter 9).
[30] W.-Y. Yu, W.-X. Tu, H.H.-F. Liu, Langmuir 15 (1999) 6.
[31] G.S. Chai, S.B. Yoon, J.-S. Yu, J.-H. Choi, Y.-E. Sung, J. Phys. Chem. B 108 (2004) 7074.
[32] B. Fang, J.H. Kim, M.-S. Kim, J.-S. Yu, Chem. Mater. 21 (2009) 789.
[33] X.-H. Ji, X.-N. Song, J. Li, Y.-B. Bai, W.S. Yang, X.-G. Peng, J. Am. Chem. Soc. 129 (2007) 13939.
[34] R.P. Briñas, M.-H. Hu, L.-P. Qian, E.S. Lymar, J.F. Hainfeld, J. Am. Chem. Soc. 130 (2008) 975.
[35] J.R.C. Salgado, E. Antolini, E.R. Gonzalez, J. Power Sources 138 (2004) 56.